33RD INTERNATIONAL COSMIC RAY CONFERENCE, RIO DE JANEIRO 2013
THE ASTROPARTICLE PHYSICS CONFERENCE

Nuclear Charge Measurement With the AMS-02 Silicon Tracker

G.AMBROSI[1], P. AZZARELLO [1,6], R. BATTISTON[1,2], J.BAZO[1], B.BERTUCCI[1,3], E. CHOUMILOV[4], V.CHOUTKO[4], C.DELGADO-MENDEZ[5], M.DURANTI[1], D.D'URSO[1], E.FIANDRINI[1,3], M.GRAZIANI[1,3], M. HABIBY[6,7], S.HAINO[8], M.IONICA[1,3], I.MEREU[1,3], S.NATALE[6], F.NOZZOLI[1,9], A. OLIVA[5], M. PANICCIA[6,7], C.PIZZOLOTTO[1,9], M.POHL[6,7], D.RAPIN[6,7], P.SAOUTER[6,7], N.TOMASSETTI[10], K.WU [11,12], Z. ZHANG[13], P.ZUCCON[4].

[1] *INFN-Sezione di Perugia, I-06100 Perugia, Italy.*
[2] *INFN-TIFPA and Università di Trento, I-38123 Povo, Trento, Italy.*
[3] *Università di Perugia, I-06100 Perugia, Italy.*
[4] *Massachusetts Institute of Technology, MIT, Cambridge, Massachusetts 02139, USA.*
[5] *Centro de Investigaciones Energeticas, Medioambientales y Tecnologicas, CIEMAT, E-28040 Madrid, Spain.*
[6] *DPNC, Université de Genève, CH-1211 Genève 4, Switzerland*
[7] *Center for Astroparticle Physics, CAP, Geneva, Switzerland.*
[8] *National Central University, NCU, Chung-Li, Tao Yuan 32054, Taiwan.*
[9] *ASDC ESRIN, I-00044 Frascati, Italy.*
[10] *LPSC, Université Joseph Fourier Grenoble 1, CNRS/IN2P3, Institut Polytechnique de Grenoble, 38026 Grenoble, France.*
[11] *Beihang University, BUAA, Beijing, 100191, China.*
[12] *Institute of Physics, Academia Sinica, Nankang, Taipei 11529, Taiwan.*
[13] *Sun Yat-sen University, SYSU, Guangzhou, 510275 China.*

Pierre.Saouter@unige.ch

Abstract: The AMS-02 magnetic spectrometer was installed on the International Space Station (ISS) in May 2011 and has since then been successfully collecting data. One of its main sub-detectors, the silicon tracker, determines the trajectory and absolute charge (Z) of cosmic rays by multiple measurements of energy loss in nine layers of double sided silicon micro-strip detectors. In this contribution we describe the procedure that has been used to accurately calibrate the tracker response and optimize its performances in terms of charge resolution.

Keywords: Charged Particles, Cosmic Ray Detector, Silicon Tracker.

1 Introduction

The Alpha Magnetic Spectrometer (AMS-02) is a state-of-the art particle physics detector operating as an external module on the International Space Station since May 2011. The purpose of the experiment is to perform accurate, high-statistics, long-duration measurements of the spectra of charged cosmic rays from 0.5 GeV to few TeV energy.

The detector consists of nine layers of precision silicon tracker inside and outside the field of a permanent magnet, a transition radiation detector (TRD), four planes of time of flight counters (TOF), an array of anti-coincidence counters (ACC) surrounding the inner tracker, a ring imaging Cerenkov detector (RICH), and an electromagnetic calorimeter (ECAL). Figure 1 shows a schematic view of the AMS detector. More details on the various sub-detectors can be found in [1].

The silicon tracker is the only sub-detector that can separate positive from negative particles, hence matter from anti-matter, using the measurement of the particle magnetic rigidity (R=p/Z), and the information of up-going or down-going particle coming from TOF. On top of this crucial measurement, the tracker measures with an excellent resolution the magnitude of the charge of the traversing particle, offering up to nine independent measurements of the specific energy loss. Moreover, the single layer charge identification capability provides an important tool for tagging the nuclear fragmentation appearing at different levels in the detector. For these reasons, a precise calibration of the tracker is of essential importance for many physics topics.

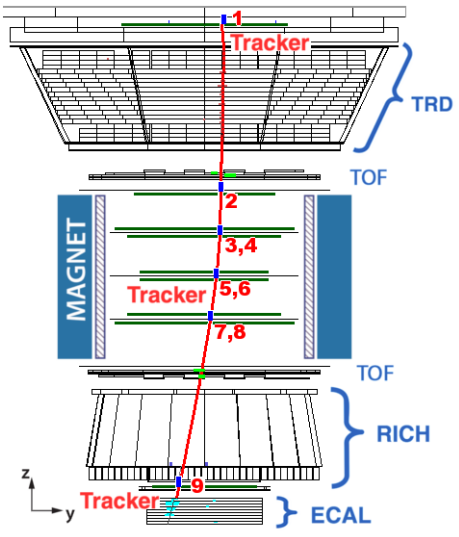

Fig. 1: The figure displays the main sub-detectors composing AMS-02, presented in the bending ($y-z$) plane. The red line corresponds to a measured low energy proton.

2 The Silicon Tracker

2.1 The Detector

The tracker system is composed of 2284 double-sided silicon micro-strip sensors, with dimensions $\sim 72 \times 41 \times 0.3\text{mm}^3$, assembled in basic functional elements called ladders. Each ladder is composed of 9 to 15 sensors, for a total of 192 ladders, and an active area of 6.75 m^2.

Each face of a sensor is implanted with metallic strips running in orthogonal directions, providing the bi-

dimensional measurement of the particle's position. The junction side (or p-side) is composed of p^+ doped strips, for an implantation (readout) pitch of 27.5 μm (110 μm); the opposite ohmic side (the n-side) has a larger implantation (readout) pitch of 104 μm (208 μm). The p and n sides are separately connected in different daisy chains to the front-end electronics. The front-end hybrid design is based on a high dynamic range 64 channel chip developed on the basis of the VA and Viking chips [2]. A total of 10(6) VA chips are used to read the signals from the p(n) sides. Details of the tracker design and the construction of sensors and ladders can be found in Refs. [3, 4].

When a particle traverses a silicon sensor, electron-hole pairs are created along the particle trajectory. Due to the electric field in the depleted area, electron and holes migrate to opposite sides. The opposite sign of the collected signals also has an impact on the VA performances which are therefore different on the two sides, in particular for what concerns saturation effects.This implies a separated calibration of the two sides (see Sec.3).

The ionization energy is proportional to the square of the particle charge ($dE/dx \propto Z^2$), therefore allowing to distinguish different nuclear species. The analog readout and the high dynamic range of the front end electronics of the ladders allow to identify nuclear species from hydrogen up to iron and above.

In the construction phase of the detector, a limited number of ladders have been exposed to several particle beams in order to evaluate their performances, in terms of position resolution but also in terms of their charge identification capabilities. A detailed description of the ladders, as well as the results of these performance studies can be found in Ref. [4].

2.2 Charge Measurement

The energy deposited in a sensor is collected by a cluster of adjacent read-out strips. The total cluster amplitude is defined as the sum of the individual cluster strip signals, which is proportional to the energy deposited in the silicon by the particle. The ADC values of the readout strips include several contributions: a constant offset (pedestal), a common noise component, the strip noise and the signal corresponding to the charge accumulated on the strip due to the passage of a particle. A threshold applied to the strip signal-to-noise ratio defines a valid signal. The calibration is performed four times per orbit when a new data acquisition run is started. Details of the calibration procedure can be found in [4].

The cluster amplitude depends on the impact position of the particle on the sensor and on its inclination, as can be seen in Figure 2 for a selected sample of helium nuclei measured by the n-side. The *Impact Point* (IP) is defined as the distance, in units of readout strip pitch, of the particle impact point on the sensor surface to the closest readout strip. For a particle impinging directly on a readout strip, $IP = 0$, while $IP = 0.5$ when the particle traverses in between two readout strips. The θ_{XZ} angle corresponds to the projection of the particle inclination onto the $x-z$ plane of AMS[1].

The observed dependence can be understood in terms of a loss of collection efficiency when a particle traverses the sensor surface in between two readout strips, while the maximum charge collection efficiency appears when

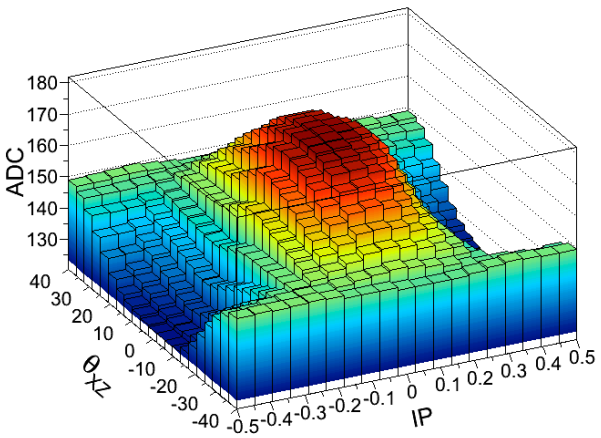

Fig. 2: Illustration of the dependence of the raw signal on the impact position of the particle and its inclination for a selected sample of helium nuclei. The maximum of collection efficiency appears when the particle traverses at vertical incidence, impinging directly on a readout strip, i.e. $IP = 0$ and $\theta_{XZ} = 0$.

the particle impacts vertically on a readout strip. For the former case, at higher inclinations, the signal tends to be distributed to a larger number of strips which partially compensates the loss of collection and attenuates the effect. The total effect can amount to differences up to more than 30% for the lighter nuclei ($Z < 6$). As the charge increases, the deposited energy is collected by an increasing number of readout strips and the effect tends to decrease.

3 Charge Equalization and Linearization

The charge resolution of the tracker is naturally degraded by a number of detector effects that need to be carefully taken into account and corrected for. In-flight calibration of the Tracker is done using the statistics accumulated over two years of operation, allowing to perform a precise equalization and linearization of the amplifier chips' responses. This is achieved using the characteristic energy deposition signature of the most abundant nuclear species.

3.1 Charge Sample Selection

To characterize the behavior of the electronics as a function of the nuclear charge Z, a selection of samples of different nuclear species is needed. This selection can be performed looking at the truncated mean (S_T) of cluster signals S_i belonging to a reconstructed particle track in the tracker :

$$S_T = \frac{\sum_{i=1}^{n} S_i - S_{max}}{n-1} \quad (1)$$

Figure 3 gives an illustration of the selection procedure, where the square root of the truncated mean calculation is used for its direct proportionality to the charge of the particle ($\sqrt{S_T} \propto Z$). Also, we use a dedicated data sample where

1. For considering the effect for the p-side measurement, the relevant angle becomes θ_{YZ}, the inclination projected on the $y-z$ plane.

the contribution of charge 1 particles has been partly suppressed.The truncated mean is fitted with a multi-gaussian function from which we extract single gaussian contributions to define 1-σ selection ranges around the peak values. This definition ensures a contamination from the $Z+1$ and $Z-1$ populations lower than 1% up to oxygen. Since the raw n-side measurement presents better performance, we also use it to define the selection ranges on the p-side.

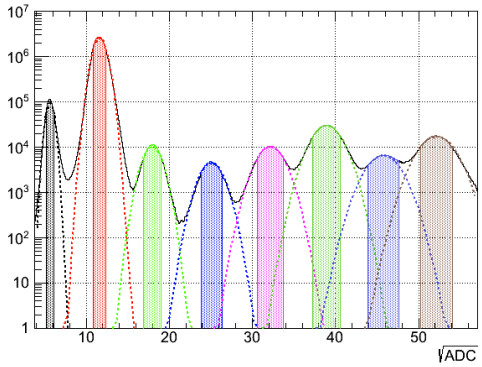

Fig. 3: A typical n-side truncated mean distribution in units of $\sqrt{ADC}$. The peaks of nuclei up to oxygen are clearly visible. The super-imposed gaussian functions are constructed from the parameters resulting from a multi-gaussian fit to the distribution.

3.2 VA Equalization

We first correct for differences in the response of the different VA chips. We fit the energy loss distributions using a Landau function convoluted with a Gaussian noise function from which we extract the Most Probable Value (MPV) to characterize the peak position of the distribution. For each one of the 3072 VA units, the MPV values are extracted for the 3 most abundant nuclear species: hydrogen, helium and carbon. We use a sample of known high quality VAs to compute reference MPV values to which all the VA responses are equalized.

Due to the loss of collection efficiency in regions between readout strips, the analysis is performed in two separated readout regions to avoid any bias in the signal estimation. The distinction is made for particles passing on or near a readout strip and for particles passing in between. The two set of MPV values obtained are used to improve the statistical power of the method as well as a cross-check to the assumption that the VA response does not depend on the impact position of the particle. The dependence with the inclination of the particle is neglected in order to save statistics. We further imposed a cut on the β of the particle to be greater than 0.97 to be free of the low energy dependence of energy loss in matter (see 3.4).

3.3 Charge Loss Correction

Once the VA responses are equalized, we can combine the statistics of the p and n-side VAs to produce 3-dimensional description plots of the type of Figure 2 for each nuclear species and each sensor side. The resolution of this description depends however on the relative abundances of the different species. Wherever statistics is sufficient, we fit with the usual Landau-Gaussian convoluted function the signal distribution in each bin of impact parameter and inclination. With the resulting MPV values, maps of the charge loss effect are created for each nuclei.

The equalization is applied to ADC signals by searching for the closest 3-dimensional point in the stored maps. Whenever a point is missing in a given map, the correction algorithm interpolates between the information of the next closest maps. In the process of correcting for this effect, the ADC scale of the deposited energy measurement is converted to nuclear charge units.

3.4 Energy Dependences

The deposited energy presents a dependence with the energy of the particle, following the Bethe-Bloch formula. The observed dependence for a proton sample measured with AMS is presented in Figure 4. We observe a significant increase of the deposited energy for low particle energies while a slow rise is also present at high energies.

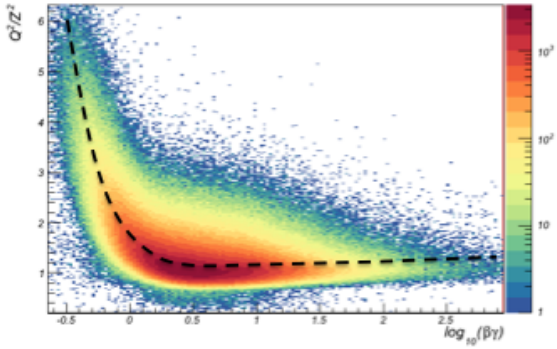

Fig. 4: Energy dependence of the proton energy loss in the silicon tracker.

We describe the energy dependence using the universal $\beta\gamma$ parameter, corresponding to the momentum over mass value of the particle (p/m). This parameter can be estimated directly from the TOF β measurement and indirectly from the tracker reconstructed rigidity (R):

$$(\beta\gamma)_{Tof} = \frac{\beta}{\sqrt{1-\beta^2}} \tag{2}$$

$$(\beta\gamma)_{Trk} = R \times \frac{Z}{m} \tag{3}$$

The rigidity estimation is used for the high energy description where its intrinsic resolution is better than TOF.

To account for the additional energy lost by the particle while traversing the AMS detector material, the correction is implemented for each layer and each sensor side, and a specific parametrization is derived for each nuclei.

3.5 Final Equalization and Linearization

After correcting for the main effects affecting the charge resolution of the tracker measurement, we observe significant residual differences in the VA chips' responses, starting around the CNO group on the p-side, and above magnesium for the n-side. This is understood in terms of specific non-linearities and saturation effects in the response curve of both sides.

We thus iterate on the equalization procedure, this time fitting the signal distribution for each single VA with no

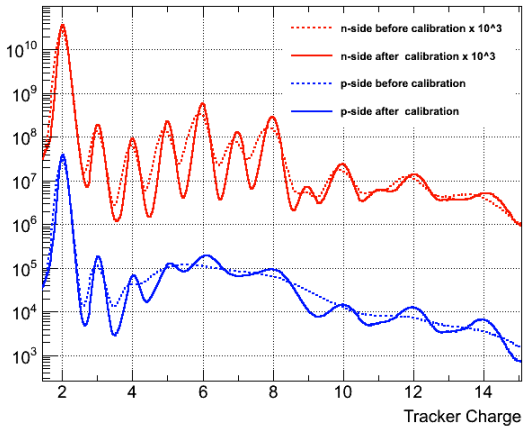

Fig. 5: Overall improvement in the tracker charge measurement after applying the calibration, for the n-side (red) and p-side (blue) measurements. The effect is shown up to silicon (Z=14) where the n-side saturation starts degrading the measurement.

restriction on impact regions nor on energy since we have corrected for these effects. Without these limitations, the accumulated statistics is enough to extract MPV values for each single nucleus up to Iron, and perform the new calibration to the unit charge values.

4 Charge Identification Performances

Figure 5 shows the overall improvement in the p (blue) and n-side (red) charge measurements before and after all the calibration steps are applied. The improvement in resolution is most significant for charges up to magnesium, where the n-side response starts saturating, implying a natural degradation of the measurement. For the p-side, a charge distinction power is even achieved in the saturation region around the CNO group.

It is possible to profit from both the p and n-side measurements to improve the overall charge identification power. The two measurements are combined using a weighted sum, where the weights are related to the specific resolutions, depending on the number of points used in the truncated mean computation. The final combined estimator is shown in Figure 6 (top plot) over the full range of charges. Nuclei up to silicon (Z=14) can clearly be separated. Above, nuclei with even charge number can also be distinguished. The iron peak itself is clearly visible due to its natural higher abundance compared to neighboring charges.

For the combined measurement, we reach a resolution at the level of 0.1 charge units (c.u.) for carbon and lower than 0.3 c.u. up to silicon. This is shown in Figure 6 (bottom plot) where the quoted values are obtained by fitting single charge distributions with a simple gaussian function for two different cases : a minimum number of 8 layers entering the measurement (magenta curve) and the general case with at least 4 layers (black curve).

At 99% selection efficiency, the contamination from neighboring charges is estimated to be lower than 10^{-4} up to oxygen (Z=8) with a mis-identification probability for carbon lower than 10^{-6}.

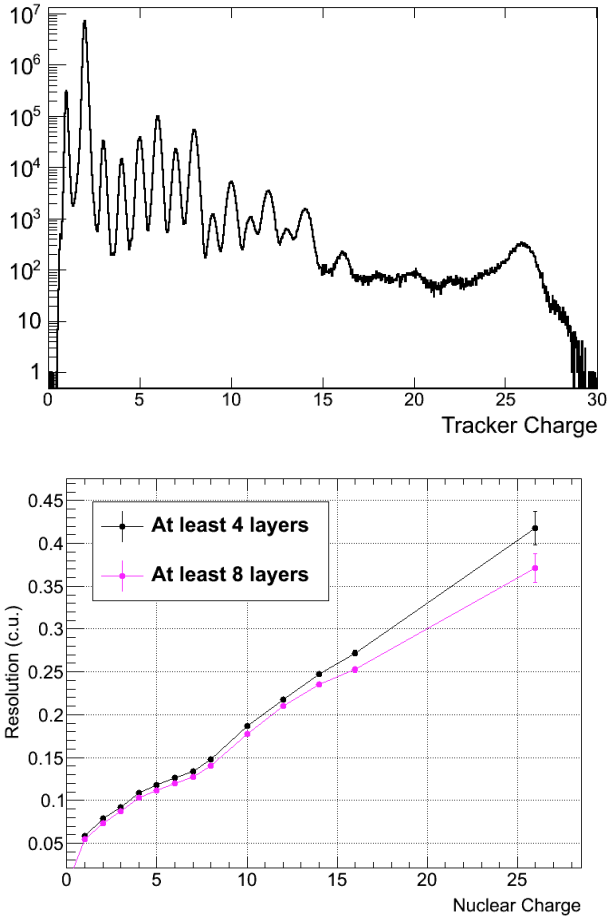

Fig. 6: Top : Final tracker charge estimator for the combined p and n-side measurements. Bottom : Combined charge estimator resolution (in charge units) for nuclei up to silicon.

5 Conclusion

The fluxes of completely ionized nuclei in cosmic rays, as well as secondary-to-primary ratios such as the B/C ratio, are important information to constraint models of production, acceleration and propagation of cosmic rays in the galaxy.

In this contribution, a procedure to improve the charge identification performances of the AMS-02 silicon tracker has been presented. After correcting for the most relevant effects degrading the charge measurement, we reach an excellent overall charge separation power with a mis-identification probability for carbon lower than 10^{-6}.

References

[1] M. Aguilar et. al., (AMS collaboration), Phys. Rev. Lett. 110, 141102 (2013), and references therein.
[2] E. Nygard, et al., Nucl. Instr. and Meth. A 301 (1991) 506.
[3] Ph. Azzarello,Test and production of the AMS-02 silicon tracker detectors, University of Geneva Thesis, 2004, unpublished.
[4] J. Alcaraz, and al., The alpha magnetic spectrometer silicon tracker: Performance results with protons and helium nuclei, Nucl. Instr. and Meth. A 593 (2008) 376.
[5] C. Amsler et al., Physics Letters B667 (2008) 1.